Protected Noble Metal Clusters

DOI: 10.1002/ange.201311177

# Balancing the Rate of Cluster Growth and Etching for Gram-Scale Synthesis of Thiolate-Protected $Au_{25}$ Nanoclusters with Atomic Precision**

*Xun Yuan, Bin Zhang, Zhentao Luo, Qiaofeng Yao, David Tai Leong, Ning Yan,* and Jianping Xie**

***Abstract:*** *We report a NaOH-mediated $NaBH_4$ reduction method for the synthesis of mono-, bi-, and tri-thiolate-protected $Au_{25}$ nanoclusters (NCs) with precise control of both the Au core and thiolate ligand surface. The key strategy is to use NaOH to tune the formation kinetics of Au NCs, i.e., reduce the reduction ability of $NaBH_4$ and accelerate the etching ability of free thiolate ligands, leading to a well-balanced reversible reaction for rapid formation of thermodynamically favorable $Au_{25}$ NCs. This protocol is facile, rapid ($\leq$ 3 h), versatile (applicable for various thiolate ligands), and highly scalable (>1 g Au NCs). In addition, bi- and tri-thiolate-protected $Au_{25}$ NCs with adjustable ratios of hetero-thiolate ligands were easily obtained. Such ligand precision in molecular ratios, spatial distribution and uniformity resulted in richly diverse surface landscapes on the Au NCs consisting of multiple functional groups such as carboxyl, amine, and hydroxy. Analysis based on NMR spectroscopy revealed that the hetero-ligands on the NCs are well distributed with no ligand segregation. The unprecedented synthesis of multi-thiolate-protected $Au_{25}$ NCs may further promote the practical applications of functional metal NCs.*

The formation process of nanoscale materials is dynamic in reaction solution, involving both the growth of nanoparticles and the digestion or etching of newly formed nanoparticles.[1] The balance of these two processes often leads to a reaction equilibrium, and nanoparticles with a minimized free energy (hence thermodynamically favorable) are finally stabilized in the solution.[2] The delicate control of both the growth and etching process of nanoparticle formation is therefore crucial for the preparation of nanoscale materials with well-controlled nanoparticle attributes, including high monodispersity in size, shape, and composition.[3] By applying this principle, here we report a new strategy for the synthesis of ultrasmall (<2 nm) gold nanoparticles or termed Au nanoclusters (NCs) with atomic precision, where a delicate balance of the rate of cluster growth and etching was created, facilitating a concurrent control of core size (Au) and ligand surface (mono-, bi- and tri-thiolates) of Au NCs in a simple and facile manner.

Thiolated Au NCs were our reaction system. Thiolated Au NCs, generally described as $Au_n(SR)_m$ ($n$ and $m$ are the number of Au atoms and thiolate ligands, respectively), are ultrasmall particles comprising of a small Au core (<2 nm) and a self-assembled thiolate ligand layer.[2b,4] This class of nanoparticles has potential applications in diverse fields like energy,[5] environment,[6] and human health.[7] Most of the applications of thiolated Au NCs are related to their interface with a particular substrate, such as substrates for catalytic reactions,[8] cells for biomedical applications,[9] and analytes for sensor development.[6] The above interfacings are predominantly dictated by the thiolate ligands on the NC surface. The interface properties of Au NCs and their subsequent behavior in practical applications can be remarkably improved by tailoring the surface of Au NCs with hetero-ligands of designed functionalities.[10] Currently, there are no generalized synthetic strategies for multi-thiolate-protected Au NCs, especially those with good control of both the Au core and hetero-ligand surface.[11] We approach this issue by returning to the reaction basics; through the most straightforward and commonly used sodium borohydride ($NaBH_4$) reduction method, in order to develop a versatile yet efficient approach for the synthesis of high-quality multi-thiolate-protected Au NCs. The $NaBH_4$ reduction method has been widely used to synthesize mono-thiolate-protected Au NCs.[12] This method involves a fast $NaBH_4$ reduction of Au ions, which often produces Au NCs with mixed sizes in the reaction solution. A slow etching process of Au NCs, typically facilitated by the addition of excess thiolate ligands, is then introduced in another reaction solution to further transform mix-sized Au NCs into monodispersed ones.[2a,13] We postulate that the cluster growth (by $NaBH_4$ reduction) and digestion (by thiol-etching) can be integrated in a single reaction solution, which can be treated as a reversible process, and a delicate manipulation of the reaction kinetics of this reversible process may lead to a better control of the NC formation.

According to this simple principle, we have developed a novel NaOH-mediated $NaBH_4$ reduction method for the synthesis of mono-, bi- and tri-thiolate-protected $Au_{25}$ NCs. The key strategy in our protocol is to introduce an optimized amount of NaOH in the reaction solution to concurrently

[*] X. Yuan, B. Zhang, Z. Luo, Q. Yao, Prof. D. T. Leong, Prof. N. Yan, Prof. J. Xie
Department of Chemical and Biomolecular Engineering
National University of Singapore
4 Engineering Drive 4, Singapore 117585 (Singapore)
E-mail: ning.yan@nus.edu.sg
chexiej@nus.edu.sg

[**] This work was financially supported by the Ministry of Education, Singapore, under Grants R-279-000-409-112, R-279-000-383-112, and R-279-000-387-112. X.Y., B.Z., Z.L., and Q.Y. acknowledge the NUS for their research scholarships.

Supporting information for this article is available on the WWW under http://dx.doi.org/10.1002/anie.201311177.

  

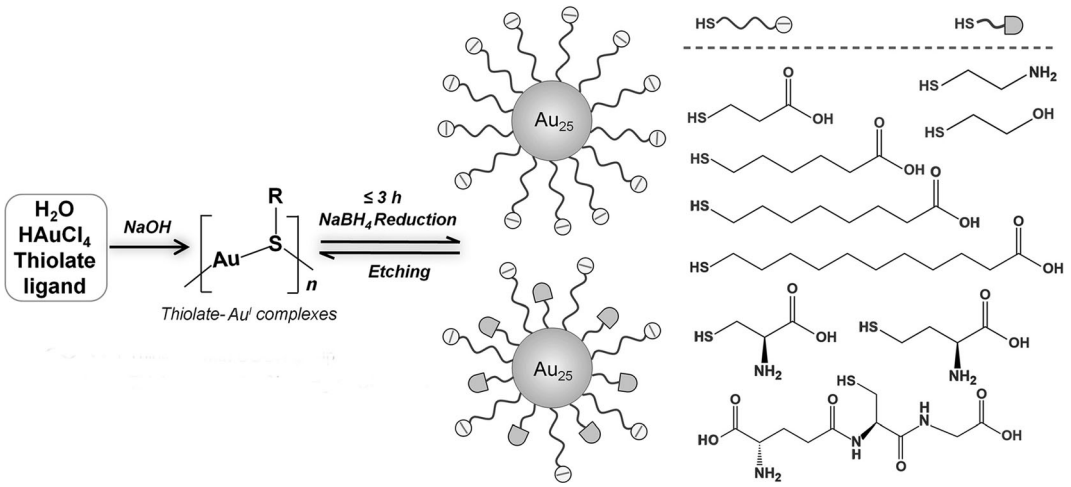


***Scheme 1.*** NaOH-mediated $NaBH_4$ reduction method for the synthesis of thiolated $Au_{25}$ NCs.

decrease the reduction ability of $NaBH_4$ (slow down the rate of the forward reaction, Scheme 1) and increase the etching ability of free thiolate ligands (push up the rate of the backward reaction, Scheme 1), leading to a well-balanced reversible reaction for NC formation, which could rapidly achieve a reaction equilibrium and result in the formation of thermodynamically favorable $Au_{25}$ NCs.

Our synthetic protocol is simple and involves two steps in a one-pot manner. As shown in Scheme 1, the first step was the introduction of NaOH to the mixture of $HAuCl_4$ and thiolate ligands to regulate the formation of thiolate-$Au^{I}$ complexes. Thereafter, an aqueous $NaBH_4$ solution was added to initiate the reduction of thiolate-$Au^{I}$ complexes, leading to the formation of Au NCs. The key step in our strategy is the introduction of an optimized amount of NaOH in the reaction solution, which could simultaneously retard the self-hydrolysis of $NaBH_4$ and enhance the etching ability of thiolate ligands. It is well-documented that hydrogen ion plays a vital role in the self-hydrolysis of $NaBH_4$,[14] and in the presence of NaOH, the reduction ability of $NaBH_4$ could be largely inhibited. On the other hand, the etching ability of thiolate ligands could be enhanced by the deprotonation of thiol groups in alkaline solution, leading to the formation of thiolates, which show stronger affinity with Au atoms on the NC surface.[15] The weakened reduction together with the enhanced etching/digestion rapidly made possible an equilibrium of the reaction and thiolated $Au_{25}$ NCs were formed in a very short period of 3 h.

As a proof-of-concept, we chose 6-mercaptohexanoic acid (MHA) as a model ligand. The as-synthesized MHA-Au NCs were first examined by UV/Vis spectroscopy. As shown in Figure 1 a, the raw NC product exhibited four distinct absorption peaks at 440, 552, 670, and 760 nm, which correspond well to the characteristic absorption of thiolated $Au_{25}$ NCs.[4a,12b] The well-defined absorption spectrum also suggests a very high quality of MHA-$Au_{25}$ NCs in our raw

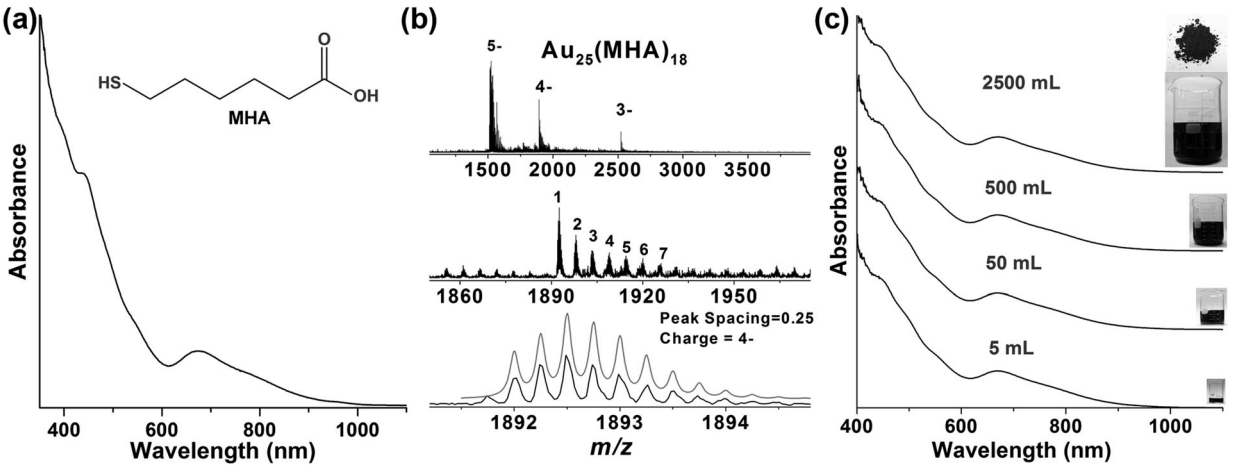


***Figure 1.*** a) UV/Vis absorption and b) ESI mass spectra of the as-synthesized MHA-$Au_{25}$ NCs. b) Broad spectrum of $Au_{25}(MHA)_{18}$ (top), zoom-in spectrum of $[Au_{25}(MHA)_{18}-3\,H]^{4-}$ (middle), and isotope pattern of $[Au_{25}(MHA)_{18}-3\,H]^{4-}$ (bottom, the gray line is the theoretical isotope pattern). In the middle panel, peak 1 corresponds to $[Au_{25}(MHA)_{18}-3\,H]^{4-}$, and the other peaks (2–7) are from the successive coordination of [+Na−H] of peak 1. c) UV/Vis absorption spectra and photographs (insets) of the as-synthesized MHA-$Au_{25}$ NCs with a gradually increased volume from 5 to 2500 mL.

product. By electrospray ionization mass spectrometry (ESI-MS), we observed three sets of intense peaks at $m/z$ 1514, 1892, and 2524 in the range of 1000–4000, which can be assigned to $[Au_{25}(MHA)_{18}-4H]^{5-}$, $[Au_{25}(MHA)_{18}-3H]^{4-}$, and $[Au_{25}(MHA)_{18}-2H]^{3-}$, respectively. The detailed assignments are presented in the middle and bottom panels of Figure 1b. Transmission electron microscopy (TEM) images (Figure S1 in the Supporting Information) suggest that the as-synthesized $Au_{25}(MHA)_{18}$ NCs were $<1.5$ nm in size. The oxidation state of Au in $Au_{25}(MHA)_{18}$ NCs was between 0 and 1 as determined by X-ray photoelectron spectroscopy (XPS, Figure S2). This value was in good agreement with several previous publications.[4a,12c]

Our protocol is facile and robust. For example, a variety of both precursor concentrations and ligand-to-Au ratios can be used to synthesize high-quality $Au_{25}$ NCs. As shown in Figures S3 and S4, the absorption spectra of MHA-Au NCs synthesized by using different concentrations of thiolate-$Au^I$ complexes (from 1 to 3 mM) and different ligand-to-Au ratios (from 1.5:1 to 4.0:1) were nearly identical. In addition, the simple one-pot manner of our protocol also transferred to excellent process scalability; about 1.3 g MHA-$Au_{25}$ NCs can be obtained in a single batch by using 2.5 L reaction solution and a 2 mM Au ion precursor (Figure 1c).

Our synthesis strategy is fairly generic and can be easily adapted to synthesize $Au_{25}$ NCs protected by other thiolate ligands. We have shown its versatility with thiol-containing alkanoic acids including $C_3$-chain 3-mercaptopropionic acid (MPA), $C_8$-chain 8-mercaptooctanoic acid (MOA), and $C_{11}$-chain 11-mercaptoundecanoic acid (MUA). All systems produced high-quality $Au_{25}$ NCs as suggested by their absorption spectra (Figure 2a), which were identical to that of MHA-$Au_{25}$ NCs (Figure 1a). ESI-MS spectra (Figure 2b) suggest their cluster formulas to be $Au_{25}(MPA)_{18}$, $Au_{25}(MOA)_{18}$, and $Au_{25}(MUA)_{18}$, respectively. The enlarged ESI-MS spectra and isotope patterns of MPA-, MOA-, and MUA-$Au_{25}$ NCs were presented in Figure S5. Moreover, more complicated thiol-containing amino acids or peptides, such as cysteine (Cys), homocysteine (HCys), and glutathione (GSH), can also be applied to synthesize high-quality $Au_{25}$ NCs (Figure S6).

One salient feature of the NaOH-mediated $NaBH_4$-reduction method is that it enables rational synthesis of thiolated $Au_{25}$ NCs with different thiolate ligand combinations. For example, the long thiol-containing alkanoic acids (e.g., MOA and MHA) collocating with short thiol-containing alkanoic acid, amine, or alcohol, such as MPA, cysteamine (Cystm), and 2-mercaptoethanol (MetH), produced bi-thiolate-protected $Au_{25}$ NCs with a high monodispersity in both the Au core and thiolate ligands. As shown in Figure 2c, by adding the same amount of two thiolate ligands into the solution whilst keeping the other reaction conditions the same, the as-synthesized MOA/MPA-Au NCs (black line), MHA/Cystm-Au NCs (blue line), MHA/MetH-Au NCs (red line) showed a typical UV/Vis absorption feature of thiolated $Au_{25}$ NCs. It should be pointed out that the absorption peak at 980 nm of MHA/Cystm-Au NCs and MHA/MetH-Au NCs was probably due to the surface charge difference of the NCs. The ESI-MS spectra (Figure 2d) clearly assigned $Au_{25}(MOA)_{10}(MPA)_8$ (black line), $Au_{25}(MHA)_{10}(Cystm)_8$ (blue line), and $Au_{25}(MHA)_9(MetH)_9$ (red line) to the as-synthesized MOA/MPA-, MHA/Cystm-, and MHA/MetH-Au NCs, respectively. Their enlarged ESI-MS spectra as well as isotope patterns can be found in Figure S7. Prominently, the proportions of two hetero-ligands on the NC surface can also be finely tuned by changing the feeding ratios of two thiolate ligands at the start of synthesis. As shown in Figure S8–S10, $Au_{25}$ NCs protected by hetero-ligands with various ratios—MOA/MPA (from 16:2, 14:4, 13:5 to 8:10), MHA/Cystm (from 14:4, 13:5, 11:7 to 10:8), and MHA/MetH (from 16:2, 13:5, 11:7 to 7:11) can be readily achieved by changing the feeding ligand ratios from 1.75:0.25, 1.5:0.5, 1.25:0.75 to 0.75:1.25. Furthermore, tri-thiolate-protected $Au_{25}$ NCs with adjustable ligand proportions can also be synthesized. A series of MOA/MPA/Cystm-$Au_{25}$ NCs (Figure S11) such as $Au_{25}(MOA)_{13}(MPA)_1(Cystm)_4$, $Au_{25}(MOA)_{11}(MPA)_2(Cystm)_5$, $Au_{25}(MOA)_{10}(MPA)_2(Cystm)_6$, and $Au_{25}(MOA)_8(MPA)_3(Cystm)_7$ were successfully synthesized. It should be mentioned that the protocol was only applicable to those thiolate ligands with different activities where a spontaneous optimization of hetero-ligands on the NC surface can occur. If two ligands with similar chemical activities, such as Cys and HCys, were used to synthesize Au NCs, a mixture of $Au_{25}(Cys)_x(HCys)_{18-x}$ NCs (where $x=2$ to 9) were obtained (Figure S12).

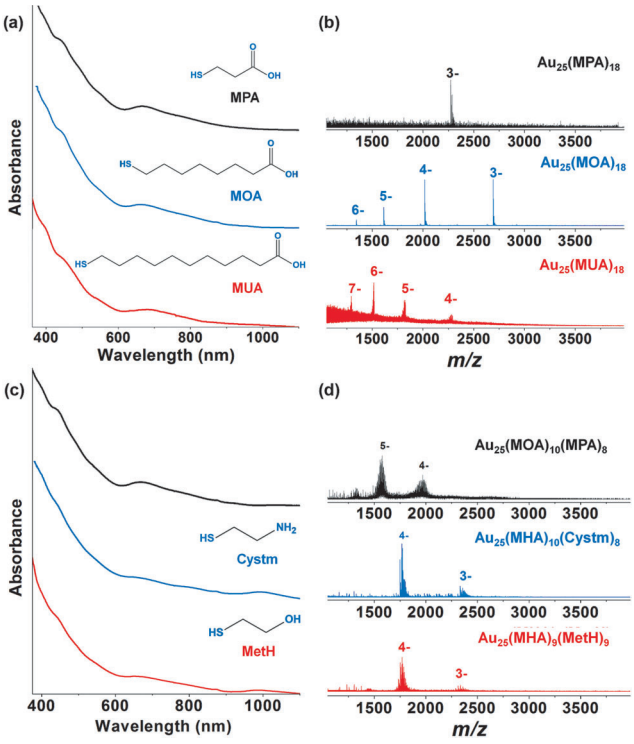


***Figure 2.*** a) UV/Vis absorption and b) ESI mass spectra of the as-synthesized mono-thiolate-protected $Au_{25}$ NCs: MPA-$Au_{25}$ NCs (black line); MOA-$Au_{25}$ NCs (blue line); and MUA-$Au_{25}$ NCs (red line). c) UV/Vis absorption and d) ESI mass spectra of the as-synthesized bi-thiolate-protected $Au_{25}$ NCs: MOA/MPA-$Au_{25}$ NCs (black line); MHA/Cystm-$Au_{25}$ NCs (blue line); and MHA/MetH-$Au_{25}$ NCs (red line).

Without the addition of NaOH, only polydisperse Au NCs were obtained after 3 h of reaction (Figure S13). To better understand the NaOH-mediated formation process of $Au_{25}$ NCs, a time-resolved evolution of absorption of MHA-$Au_{25}$ NCs was recorded. As shown in Figure S14, the solution color after $NaBH_4$ addition gradually changed from colorless (0 min), light yellow (2 to 4 min), light brown (8 min), to brown (10 min). The color changes were also reflected in their UV/Vis absorption spectra (Figure S14). In stark contrast, without the addition of NaOH, the reduction of thiolate-$Au^I$ complexes by $NaBH_4$ was much faster, which was completed in 1 min (Figure S13). This data clearly suggests that slower reduction kinetics by $NaBH_4$ was achieved in the presence of NaOH. Furthermore, from 20 min onwards, the UV/Vis absorption spectra of Au NCs began to show characteristic absorption peaks of thiolated $Au_{25}$ NCs (440, 552, and 670 nm), and the absorbance at 670 nm of the NCs increased from 20 to 180 min. Such rapid formation of $Au_{25}$ NCs implies a fast size-focusing process.

We thus reasoned that NaOH plays two major roles in our protocol: 1) NaOH can slow down the reduction rate of Au NCs through effectively retarding the hydrolysis of $NaBH_4$; and 2) NaOH can regulate the interaction between Au and thiolate ligands. The second role was further evidenced by two control experiments. First, the cloudy solution of thiolate-$Au^I$ complexes with obvious solid precipitates became transparent and the strong scattering in solution disappeared upon the addition of NaOH (Figure S15), indicating that NaOH can assist the dispersion of thiolate-$Au^I$ complexes possibly by embarking sufficient surface charges for thiolate-$Au^I$ complexes. Second, the etching rate of Au NCs (from brown to colorless) by excess thiol ligands was faster in the presence of NaOH (Figure S16), suggesting that the deprotonated thiolate ligands have stronger interaction with Au atoms.

NMR spectroscopy was then applied to probe the structural features of the $Au_{25}$ NCs. First, the $^1H$–$^{13}C$ homonuclear correlation (COSY), heteronuclear single quantum correlation (HSQC) spectra of $Au_{25}(MHA)_{18}$ NCs were recorded and satisfactorily assigned (Figure S17). Two distinct chemical environments of MHA ligands on the NCs, with a ligand ratio close to 2:1, were unambiguously identified. This indicates there are two binding modes for the thiolate ligands in the NCs, i.e., the interior binding mode where 12 thiolates connect the icosahedron and the exterior Au shell, and the exterior binding mode where each of the remaining 6 ligands connects to a pair of exterior Au atoms, which is in full agreement with previous studies.[16,17]

For $Au_{25}$ NCs with hetero-thiolate ligands, it is crucial to reveal the ligand distribution on the NC surface as it is closely related to the surface-related properties of NCs.[18] The two ligands on bi-thiolate-protected Au NCs may randomly adopt one of the two binding modes, or one ligand preferentially adopts one mode whereas the second ligand adopts the other. To clarify this, $^1H$ and COSY experiments with $Au_{25}(MHA)_9$-$(MetH)_9$ NCs were performed (Figure 3a). By comparing with the $^1H$ NMR spectrum of $Au_{25}(MHA)_{18}$ NCs, three additional peaks were assigned as the proton signals from $H_a$ and $H_b$ on MetH ligands, based on $^1H$–$^1H$ COSY patterns. The splitting of $H_1$ and $H_a$ proton signals into two pairs of peaks

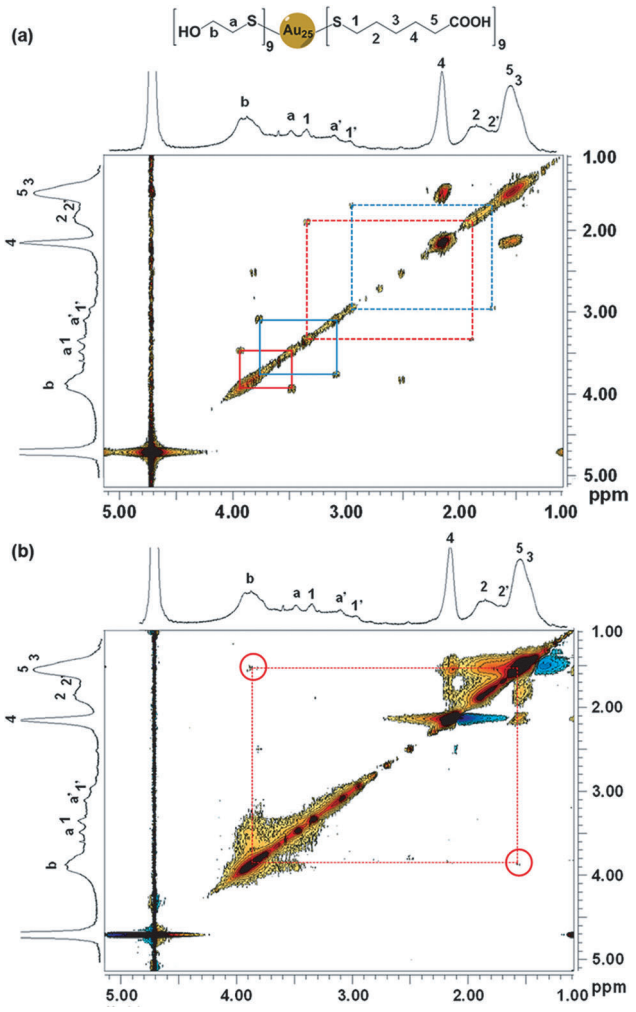


***Figure 3.*** 2-D NMR spectra of $Au_{25}(MHA)_9(MetH)_9$: a) $^1H$–$^1H$ COSY spectrum and b) $^1H$–$^1H$ NOESY spectrum. The red cycle indicates the NOESY cross peaks.

(Figure 3, labeled as 1, 1′, and a, a′) indicates that MHA and MetH ligands are both adopting two binding modes on the $Au_{25}$ NCs, ruling out the possibility of preferential ligand binding.

Another issue for bi-thiolate-protected Au NCs is that whether the binary mixtures of ligands are well-mixed or segregated into domains (such as Janus NCs, see Figure S18 for graphic representations). For random mixtures, two types of ligands are in close contact with each other, whereas for NCs bearing ligand domains such contact is significantly reduced. Nuclear Overhauser enhancement spectroscopy (NOESY), which would exhibit cross-peaks in the spectrum arising from space coupling between nuclear spins that are close enough in proximity (typically $< 0.4$ nm), is an ideal tool to differentiate these two scenarios.[10a,19] The $Au_{25}(MHA)_9$-$(MetH)_9$ NCs show clear NOESY cross-peaks between $H_b$ on MetH and $H_5$ on MHA (Figure 3b), probably through hydrogen bond interaction between OH and COOH groups from two adjacent MetH and MHA ligands. As such, the NOESY analysis strongly suggests that the two types of ligands are well mixed at the molecular level. COSY and

NOESY spectra of $Au_{25}(MHA)_{10}(Cystm)_8$ NCs were also recorded and analyzed (Figure S19), further corroborating the above mentioned structural features of $Au_{25}$ NCs synthesized by the NaOH-mediated $NaBH_4$ reduction method.

In summary, we have developed a NaOH-mediated $NaBH_4$ reduction strategy for controlled synthesis of atomically precise thiolated $Au_{25}$ NCs with various thiolate ligands. Our method utilized NaOH to balance the rate of the cluster growth and etching during NC formation, enabling a fast size-focusing process in a well-controlled manner, which generates high-quality $Au_{25}$ NCs in a short reaction period. The protocol and products developed in this study are important not only because they provide a rapid ($\leq 3$ h), simple, versatile (applicable for various thiolate ligands), robust, and scalable ($>1$ g) protocol for thiolated $Au_{25}$ NCs, but more importantly because they exemplify an efficient approach in the rational syntheses of multi-thiolate-protected $Au_{25}$ NCs with atomic precision. The proportions of hetero-thiolate ligands on the NC surface can be finely tuned and precisely controlled. 2-D NMR analysis revealed that the NC core adopts a classical two shell structure and the hetero-thiolate ligands are randomly distributed over the entire NC surface. We hope this study could shed some light on the development of novel synthetic strategies for noble metal NCs and promote the advances of noble metal NCs in both fundamental studies and practical applications.

Received: December 24, 2013
Published online: March 24, 2014

**Keywords:** nanoparticles · noble metal clusters · surface chemistry · synthesis (inorg.) · thiolate

[1] a) H. Chen, L. Shao, Q. Li, J. Wang, *Chem. Soc. Rev.* **2013**, *42*, 2679 – 2724; b) A. Vaneski, A. S. Susha, J. Rodríguez-Fernández, M. Berr, F. Jäckel, J. Feldmann, A. L. Rogach, *Adv. Funct. Mater.* **2011**, *21*, 1547 – 1556; c) Z. Lu, Y. Yin, *Chem. Soc. Rev.* **2012**, *41*, 6874 – 6887.

[2] a) R. Jin, H. Qian, Z. Wu, Y. Zhu, M. Zhu, A. Mohanty, N. Garg, *J. Phys. Chem. Lett.* **2010**, *1*, 2903 – 2910; b) H. Qian, M. Zhu, Z. Wu, R. Jin, *Acc. Chem. Res.* **2012**, *45*, 1470 – 1479; c) Y. Negishi, N. K. Chaki, Y. Shichibu, R. L. Whetten, T. Tsukuda, *J. Am. Chem. Soc.* **2007**, *129*, 11322 – 11323.

[3] a) S. V. Kershaw, A. S. Susha, A. L. Rogach, *Chem. Soc. Rev.* **2013**, *42*, 3033 – 3087; b) W. Ni, X. Kou, Z. Yang, J. Wang, *ACS Nano* **2008**, *2*, 677 – 686; c) X. Guo, Q. Zhang, Y. Sun, Q. Zhao, J. Yang, *ACS Nano* **2012**, *6*, 1165 – 1175; d) Y. Liu, J. Goebl, Y. Yin, *Chem. Soc. Rev.* **2013**, *42*, 2610 – 2653; e) Q. Zhang, J. Xie, J. Liang, J. Y. Lee, *Adv. Funct. Mater.* **2009**, *19*, 1387 – 1398; f) J. Huang, Y. Zhu, M. Lin, Q. Wang, L. Zhao, Y. Yang, K. X. Yao, Y. Han, *J. Am. Chem. Soc.* **2013**, *135*, 8552 – 8561; g) J. Yang, J. Y. Ying, *Nat. Mater.* **2009**, *8*, 683 – 689.

[4] a) Y. Negishi, K. Nobusada, T. Tsukuda, *J. Am. Chem. Soc.* **2005**, *127*, 5261 – 5270; b) Y. Yu, Q. Yao, Z. Luo, X. Yuan, J. Y. Lee, J. Xie, *Nanoscale* **2013**, *5*, 4606 – 4620; c) Z. Luo, X. Yuan, Y. Yu, Q. Zhang, D. T. Leong, J. Y. Lee, J. Xie, *J. Am. Chem. Soc.* **2012**, *134*, 16662 – 16670; d) Y. Yu, Z. Luo, D. M. Chevrier, D. T. Leong, P. Zhang, D. Jiang, J. Xie, *J. Am. Chem. Soc.* **2014**, *136*, 1246 – 1249.

[5] Y. S. Chen, H. Choi, P. V. Kamat, *J. Am. Chem. Soc.* **2013**, *135*, 8822 – 8825.

[6] X. Yuan, Z. Luo, Y. Yu, Q. Yao, J. Xie, *Chem. Asian J.* **2013**, *8*, 858 – 871.

[7] a) C. Zhou, G. Hao, P. Thomas, J. Liu, M. Yu, S. Sun, O. K. Öz, X. Sun, J. Zheng, *Angew. Chem.* **2012**, *124*, 10265 – 10269; *Angew. Chem. Int. Ed.* **2012**, *51*, 10118 – 10122; b) C. Zhou, M. Long, Y. Qin, X. Sun, J. Zheng, *Angew. Chem.* **2011**, *123*, 3226 – 3230; *Angew. Chem. Int. Ed.* **2011**, *50*, 3168 – 3172; c) D. Chen, Z. Luo, N. Li, J. Y. Lee, J. Xie, J. Lu, *Adv. Funct. Mater.* **2013**, *23*, 4324 – 4331; d) X. Zhang, J. Chen, Z. Luo, D. Wu, X. Shen, S. Song, Y. Sun, P. Liu, J. Zhao, S. Huo, S. Fan, F. Fan, X.-J. Liang, J. Xie, *Adv. Healthcare Mater.* **2014**, *3*, 133 – 141.

[8] a) Y. Zhu, H. Qian, B. A. Drake, R. Jin, *Angew. Chem.* **2010**, *122*, 1317 – 1320; *Angew. Chem. Int. Ed.* **2010**, *49*, 1295 – 1298; b) M. S. Devadas, K. Kwak, J.-W. Park, J.-H. Choi, C.-H. Jun, E. Sinn, G. Ramakrishna, D. Lee, *J. Phys. Chem. Lett.* **2010**, *1*, 1497 – 1503; c) H. Tsunoyama, H. Sakurai, Y. Negishi, T. Tsukuda, *J. Am. Chem. Soc.* **2005**, *127*, 9374 – 9375.

[9] a) J. Yu, S. Choi, R. M. Dickson, *Angew. Chem.* **2009**, *121*, 324 – 326; *Angew. Chem. Int. Ed.* **2009**, *48*, 318 – 320; b) S. Choi, R. M. Dickson, J. Yu, *Chem. Soc. Rev.* **2012**, *41*, 1867 – 1891; c) L. Shang, S. Dong, G. U. Nienhaus, *Nano Today* **2011**, *6*, 401 – 418.

[10] a) X. Liu, M. Yu, H. Kim, M. Mameli, F. Stellacci, *Nat. Commun.* **2012**, *3*, 1182; b) M. Yu, C. Zhou, J. Liu, J. D. Hankins, J. Zheng, *J. Am. Chem. Soc.* **2011**, *133*, 11014 – 11017.

[11] a) Y. Niihori, M. Matsuzaki, T. Pradeep, Y. Negishi, *J. Am. Chem. Soc.* **2013**, *135*, 4946 – 4949; b) Z. Tang, D. A. Robinson, N. Bokossa, B. Xu, S. Wang, G. Wang, *J. Am. Chem. Soc.* **2011**, *133*, 16037 – 16044; c) V. R. Jupally, R. Kota, E. V. Dornshuld, D. L. Mattern, G. S. Tschumper, D.-e. Jiang, A. Dass, *J. Am. Chem. Soc.* **2011**, *133*, 20258 – 20266.

[12] a) Y. Li, O. Zaluzhna, B. Xu, Y. Gao, J. M. Modest, Y. J. Tong, *J. Am. Chem. Soc.* **2011**, *133*, 2092 – 2095; b) M. Zhu, E. Lanni, N. Garg, M. E. Bier, R. Jin, *J. Am. Chem. Soc.* **2008**, *130*, 1138 – 1139; c) X. Yuan, Y. Yu, Q. Yao, Q. Zhang, J. Xie, *J. Phys. Chem. Lett.* **2012**, *3*, 2310 – 2314.

[13] M. Zhu, H. Qian, R. Jin, *J. Am. Chem. Soc.* **2009**, *131*, 7220 – 7221.

[14] a) M. M. Kreevoy, J. E. C. Hutchins, *J. Am. Chem. Soc.* **1972**, *94*, 6371 – 6376; b) A. Gonçalves, P. Castro, A. Novais, V. R. Fernandes, C. M. Rangel, H. Matos, *Chem. Eng. Trans.* **2007**, *12*, 243 – 247.

[15] a) S. Miranda-Rojas, A. Munoz-Castro, R. Arratia-Perez, F. Mendizabal, *Phys. Chem. Chem. Phys.* **2013**, *15*, 20363 – 20370; b) S. Letardi, F. Cleri, *J. Chem. Phys.* **2004**, *120*, 10062 – 10068.

[16] a) M. Zhu, C. M. Aikens, F. J. Hollander, G. C. Schatz, R. Jin, *J. Am. Chem. Soc.* **2008**, *130*, 5883 – 5885; b) M. W. Heaven, A. Dass, P. S. White, K. M. Holt, R. W. Murray, *J. Am. Chem. Soc.* **2008**, *130*, 3754 – 3755.

[17] a) Z. Wu, C. Gayathri, R. R. Gil, R. Jin, *J. Am. Chem. Soc.* **2009**, *131*, 6535 – 6542; b) Z. Wu, R. Jin, *ACS Nano* **2009**, *3*, 2036 – 2042.

[18] a) Q. Xu, X. Kang, R. A. Bogomolni, S. Chen, *Langmuir* **2010**, *26*, 14923 – 14928; b) A. Walther, A. H. E. Müller, *Chem. Rev.* **2013**, *113*, 5194 – 5261; c) A. Ghosh, S. Basak, B. H. Wunsch, R. Kumar, F. Stellacci, *Angew. Chem.* **2011**, *123*, 8046 – 8051; *Angew. Chem. Int. Ed.* **2011**, *50*, 7900 – 7905.

[19] S. Pradhan, L. Brown, J. Konopelski, S. Chen, *J. Nanopart. Res.* **2009**, *11*, 1895 – 1903.

  